Int. J. Heat Mass Transfer. Vol. 11, pp. 1695–1713. Pergamon Press 1968. Printed in Great Britain

GASEOUS FILM COOLING AT VARIOUS DEGREES OF HOT-GAS ACCELERATION AND TURBULENCE LEVELS

L. W. CARLSON and E. TALMOR

Research Division, Rocketdyne, A Division of North American Rockwell Corporation, Canoga Park, California, U.S.A.

(*Received* 2 *October* 1967 *and in revised form* 24 *January* 1968)

Abstract—An experimental and analytical investigation of gaseous film cooling at various rates of hot-gas acceleration and variable free-stream turbulence intensity is presented. The acceleration rate was varied through the convergence angle (0, 30, 45 and 60°) and the free-stream turbulence intensity (3·2–22 per cent) was varied by cross-flow grids upstream of the film coolant slot. The hot-gas stream consisted of 1000°F nitrogen with ambient temperature (70°F) nitrogen used as film coolant.

Quantitative results as to detrimental effects of increased free-stream turbulence and wall convergence angle on film cooling effectiveness along converging walls are given. Correlation of the data is accomplished in a form suggested by a newly derived mixing model, which considers compressibility and allows for a variable degree of mixing.

NOMENCLATURE

a, mixing coefficient, equation (6);
c_p, specific heat at constant pressure;
h, heat-transfer coefficient, $= q/(T_{aw} - T_w)$;
K, coefficient of proportionality in equation (2);
K_1, constant in equation (4);
k, thermal conductivity;
L, test section width unless noted otherwise;
m, generally mass flowrate; viscosity-temperature exponent ($\mu \sim T^m$) in equation (16);
Ma, Mach number;
Nu, Nusselt number;
Pr, Prandtl number;
p, pressure;
q, heat flux;
Re, Reynolds number;
s, film-coolant slot height;
T, absolute temperature;
t, elapsed time;
U, transformed velocity defined in conjunction with equation (8);
u, velocity in the x direction;
u', velocity fluctuation;
X, film cooling parameter for non-accelerating flow defined in conjunction with equation (2); also transformed coordinate defined in conjunction with equation (8);
X_1, generalized film cooling parameter defined in conjunction with equation (16);
x, distance from the film coolant slot along the wall; also distance from the start of convergence along the wall;
Y_1, film cooling ineffectiveness-to-effectiveness ratio, $= (1 - \eta)/\eta$.

Greek symbols

γ, specific heat ratio;
δ, velocity boundary-layer thickness in conventional coordinates;
$\bar{\delta}$, velocity boundary-layer thickness in transformed coordinate system, equation (8);
δ^*, integral thickness parameter defined in conjunction with equation (8);
η, film cooling effectiveness, $= (T_{aw} - T'_{aw})/(T_{aw} - T_{ci})$;

θ, momentum thickness in conventional coordinates;
$\bar{\theta}$, momentum thickness parameter defined in conjunction with equation (8);
μ, gas viscosity;
ν, kinematic viscosity;
ξ, wall thickness;
ρ, density;
$\bar{\tau}$, transformed shear stress defined in conjunction with equation (8).

Subscripts

aw, adiabatic wall;
bl, in the boundary layer;
c, pertaining to the film coolant;
ci, pertaining to film coolant at injection conditions;
e, local conditions along the outer edge of the boundary layer;
fc, of the film coolant;
g, pertaining to the hot gas;
hg, of the hot gas mixed with the film coolant;
o, property at stagnation conditions;
r, property at reference temperature;
s, based on s or at the film coolant slot;
w, wall;
x, based on x.

Superscripts

$'$, with film cooling.

INTRODUCTION

ROCKET engine surfaces are being exposed to extremely high, local heat fluxes as the trend toward higher chamber pressures and smaller chamber dimensions continues. Under these conditions, regenerative cooling is insufficient to prevent excessive surface temperatures because of pressure drop and wall conduction limits. The extreme heat fluxes may, however, be accommodated through the use of new materials with higher allowable operating temperatures, or by augmenting regenerative cooling with other means of cooling, e.g. film cooling.

Most of the film cooling investigations conducted to date are restricted to straight test sections and negligible free-stream turbulence intensities. In cases where hot-gas acceleration effects were considered [1, 2], the film cooling was along a non-converging side slate opposite to a converging wall rather than along the converging wall. Such data are hardly applicable for the design of film-cooled converging walls. Furthermore, the presence of a combustion-induced free-stream turbulence (particularly in short chambers) cannot be ignored.

To provide basic information for the design of film-cooled, straight and converging walls, the effectiveness of film cooling was investigated under variable conditions of free-stream turbulence intensity, hot-gas acceleration rate, approach Mach number, and film coolant flowrate. The free-stream turbulence intensity (3·2–22 per cent) was artificially induced by grids upstream of the point of film coolant injection, and the rate of hot-gas acceleration was varied through the convergence angle (30, 45 and 60°). The hot-gas stream consisted of gaseous nitrogen (1000°F at 150–450 lb/in^2) with ambient temperature (70°F) nitrogen used as film coolant.

A large amount of information was obtained concerning the effects of Mach number, turbulence, and acceleration rate upon film cooling effectiveness. Correlations of these effects are presented and discussed in the body of this paper. Preceding this discussion are sections on analytical considerations, apparatus, and procedures.

ANALYTICAL CONSIDERATIONS

General survey

The injection of a gaseous film coolant along a wall normally results in essentially two types of flow downstream of the point of film coolant injection: a wall-jet region, followed by a fully developed boundary-layer flow [3–5]. The wall-jet region consists of a potential core zone wherein the wall temperature is maintained at the film-coolant injection temperature, and a mixing zone wherein the film cooling effectiveness is a function of distance $x^{0.5}$ [4, 5]. Within the subsequent boundary-layer region the coolant and

hot-gas mixing is normally in terms of distance $x^{0.8}$ [3, 6–8].

The occurrence of both types of flow leads Spalding [4] to the correlation of film cooling effectiveness data in terms of an additive parameter representing wall-jet and boundary-layer flow conditions. However, the significance of the wall-jet region is diminished as the superficial mass velocity of the hot gas is increased with respect to that of the film coolant, i.e. at high degrees of hot-gas acceleration. For this case, the boundary-layer model for correlating film cooling data should be useful.

Most boundary-layer models [3, 6, 7] assume mixing of the film coolant with the hot gas. Only in one case [9] is the coolant assumed to exist as a discrete layer, and, as such, the model does correlate data close to the film-coolant injection point. However, empirical constants have to be introduced to allow for some degree of mixing [9].

Generally, two procedures have been used to describe the mixing process. The more common one considers the amount of hot gas mixed with the film coolant as the difference between the mass flow within the mixed boundary layer and the mass flowrate of the film coolant, i.e.

$$m_{hg} = m_{bl} - m_{fc} \tag{1}$$

where m_{bl} is calculated on the basis of hot-gas properties. A heat balance is then written between m_{hg} and m_{fc} to obtain the adiabatic wall temperature. This approach, explicit in some cases [3] and implicit in others [6, 7], leads to the following form for non-accelerating flow when (c_{p_g}/c_{p_c}) is close to unity:

$$\eta \equiv \frac{T_{aw} - T'_{aw}}{T_{aw} - T_{ci}} = \frac{K}{X} \tag{2}$$

where

$$X = \frac{Re_{g,x}^{0.8}}{Re_{c,s}} \left(\frac{k_g}{k_c}\right) \left(\frac{Pr_g}{Pr_c}\right).$$

Theoretical predictions for the value of K vary from 3·09 to 5·44 [3]. The relatively wide range for this constant results from the different assumptions made by various investigations [3, 6, 7] regarding the extent of mixing of the film coolant with the hot gas. The higher the degree of mixing the lower the constant. For complete mixing, K takes the value of 3·0.

Comparison of equation (2) to experimental results indicates that one value of K cannot correlate the data in the form of equation (2) for the entire range of X investigated. For example [10], K has to vary from a value of 3·4 at $X = 5$ to a value of 5·2 at $X = 20$.

One of the main problems in comparing various experimental results is that the free-stream or boundary-layer turbulence intensity, at least at the point of film coolant injection, is not given. The presence of free-stream turbulence is normally unintentional, but its absence cannot be ensured without actual measurements. Variation in turbulence level can be induced by the injection of the film coolant [11, 12] and/or by a high degree of hot-gas acceleration [13]. Different turbulence levels would result in various values of K in equation (1), and the higher the turbulence intensity, the closer is the approach to complete mixing of film coolant and hot gas.

The assumption of complete mixing even at negligible free-stream turbulence intensities has been successfully employed by Librizzi and Cresci [14]. This assumption has the shortcoming of implying discontinuity of temperature at the outer edge of the boundary layer [4]. However, it provides a sound basis for analysis, particularly when effects of free-stream turbulence are experimentally investigated.

Librizzi and Cresci [14] also assume no interaction between the hot-gas mass flow in the boundary layer without coolant injection and the film coolant mass flow, i.e. the amount of hot gas mixed with the film coolant is the mass flow in the boundary layer in absence of film coolant, or

$$m_{hg} = m_{bl}. \tag{3}$$

A heat balance between m_{bl} and m_{fc} then leads to the following form for nonaccelerating flow:

$$\eta = \frac{1}{1 + K_1 X} \tag{4}$$

or

$$\frac{1 - \eta}{\eta} = K_1 X$$

where X is defined in conjunction with equation (2).

With $K_1 = 0{\cdot}33$ [14], equation (4) is in good agreement with the experimental results of Nishiwaki *et al.* [15] obtained with air as the film coolant and main gas stream.

The validity of equation (3), which implied no interaction between m_{fc} and m_{bl} has recently been examined by Chapman [16]. He concludes that the direct addition of the injected film coolant to the mass in the undisturbed boundary layer is a very good approximation if m_{fc}/m_{bl} is less than 0·5.

Using a similar approach, Kutateladze and Leontev [17] obtain the following form for nonaccelerating flow when (c_{p_g}/c_{p_c}) is close to unity:

$$\eta = \frac{1}{[1 + 0{\cdot}24\, X^{5/4} (\mu_c/\mu_g)^{1/4}]^{0{\cdot}8}} \tag{5}$$

where X is defined in conjunction with equation (2). Equation (5) correlates the air–air data of Goldstein *et al.* [18, 19] markedly well, and the results of its application are very close to those of equation (4) with $K_1 = 0{\cdot}33$ [14].

For dissimilar systems, e.g. air as main stream and helium as film coolant [9, 19], equations (4) and (5) were found to be somewhat conservative [19]. Goldstein, Rask and Eckert [19] compare their air-helium results with those obtained with an air–air system, all with a porous plate as the film-coolant injection device. They report that, while the film cooling effectiveness with air injection agrees quite well with the predictions of equations (4) or (5), the film cooling effectiveness results for helium injection are considerably above these predictions. However, inspection of the run conditions involved [19] reveals that the blowing ratio $u_c\rho_c/u_g\rho_g$ for the air injection tests was an order of magnitude higher than for the helium injection tests. While the helium concentration measurements at the wall account for all the helium injected, there is no proof that this was the case with air injection. In fact, the higher blowing rates with air [19] seem to have exceeded the critical blowing parameter [20, 21] for injection through a porous plate. On this basis the improved film cooling effectiveness with helium seems to be the result of more favorable injection conditions rather than the effect of employing dissimilar gases.

Other air injection results with a porous plate [15] are in line with the air injection data of Goldstein *et al.* [18, 19]. However, the air-injection, film-cooling effectiveness data of Chin *et al.* [20] obtained with a 0·115-in slot at a 3° inclination to the main gas direction are considerably higher and in good agreement with the helium injection data of Hatch and Papell [9] at a comparable (0·125-in) slot height. Furthermore, the porous plate helium injection results of Goldstein *et al.* [19], at low gas-to-coolant temperature ratios are in excellent agreement with the 0·125-in slot, helium results of Hatch and Papell [9] at higher gas-to-coolant temperature ratios. Thus the results are inclusive as to the effect of dissimilar film coolant and main gas streams. Therefore, further investigation has been undertaken as a follow on to the present study.

Other effects heretofore not investigated or not fully covered are those of free-stream turbulence and main gas acceleration. With increasing turbulence, the amount of hot gas mixed with the film coolant can no longer be restricted to the mass flow in the boundary layer, and the imposition of hot-gas acceleration, as encountered in high-temperature combustors, calls for consideration of compressibility effects. A suitable model is derived herein and subsequently used to correlate and analyze newly obtained data.

Film cooling in compressible accelerated flow with intensified mixing

The starting point of the analysis is the contention that the amount of hot gas mixed with the film coolant is proportional to the mass flow in the boundary layer without mass addition, or

$$m_{hg} = a u_e \rho_e L(\delta - \delta^*) = a u_e \rho_e L\theta \times \left(\frac{\delta}{\theta} - \frac{\delta^*}{\theta}\right) \quad (6)$$

where a, termed mixing coefficient, may be expected to increase with distance from the film-coolant injection point and at a given position it should increase with the free-stream turbulence intensity.

Assuming a one-seventh-power velocity profile, $(\delta/\theta) = 72/7$ and $(\delta^*/\theta) = 9/7$. Substitution in equation (6) yields

$$m_{hg} = 9 a u_e \rho_e L\theta \quad (7)$$

where θ is the momentum thickness to be derived from the integral momentum equation.

In terms of a modified Stewartson coordinate system [22], the integral momentum equation for an accelerating, compressible, turbulent boundary layer on an infinite wall can be written as follows:

$$\frac{d\bar{\theta}}{dX} + \frac{1}{U_e}\frac{dU_e}{dX}(2\bar{\theta} + \delta^*) = \frac{\bar{\tau}_x}{\rho_0 U_e^2} \quad (8)$$

where

$$\bar{\theta} = \int_0^{\bar{\delta}} \left[\frac{U}{U_e} - \left(\frac{U}{U_e}\right)^2\right] dY$$

$$X = \int_0^x \frac{\rho_r \mu_r}{\rho_0 \mu_0}\sqrt{\frac{T_e}{T_0}}\,dx$$

$$U_e = \sqrt{\frac{T_0}{T_e}}\,u_e$$

$$\delta^* = \int_0^{\bar{\delta}} \left(1 - \frac{U}{U_e}\right) dY$$

$$\bar{\tau} = \frac{\rho_0 \mu_0}{\rho_r \mu_r}\left(\frac{T_0}{T_e}\right)\tau_x$$

$$Y = \sqrt{\frac{T_e}{T_0}}\int_0^y \frac{\rho}{\rho_0}\,dy.$$

With a one-seventh-power velocity profile in the boundary layer, $(\delta^*/\theta) = 1{\cdot}286$ and the shear stress is $\bar{\tau}_x/\rho_0 U_e^2 = 0{\cdot}0128\ (\nu_0/U_e\bar{\theta})^{1/4}$. Substituting in equation (8) and multiplying both sides of the equation by $(5/4)\bar{\theta}^{1/4} U_e^{115/28}\,dX$,

$$\frac{5}{4}\bar{\theta}^{1/4} U_e^{115/28}\,d\bar{\theta} + \frac{115}{28}\bar{\theta}^{5/4} U_e^{87/28}\,dU_e = 0{\cdot}0160\,\nu_0^{1/4} U_e^{27/7}\,dX \quad (9)$$

or

$$d(\bar{\theta}^{5/4} U_e^{115/28}) = 0{\cdot}0160\,\nu_0^{1/4} U_e^{27/7}\,dX.$$

Integrating and solving for $\bar{\theta}$,

$$\bar{\theta} = \frac{0{\cdot}0366\nu_0^{1/5}}{U_e^{23/7}}\left[\int_0^x U_e^{27/7}\left(\frac{T_e}{T_0}\right)^{1/2} \times \left(\frac{\rho_r \mu_r}{\rho_0 \mu_0}\right) dx\right]^{4/5}. \quad (10)$$

Writing equation (7) in the form

$$m_{hg} = 9 a U_e \rho_e L.\bar{\theta} \quad (11)$$

Substitution for $\bar{\theta}$ and slight rearrangement yield

$$m_{hg} = 0{\cdot}329\, aL\,(Re_{g,x})^{4/5}\left(\frac{\rho_e}{\rho_0}\right)^{1/5}\left(\frac{\mu_0}{\mu_e}\right)^{1/5} \times \left(\frac{T_e}{T_0}\right)^{8/7}\frac{\mu_e}{x^{4/5} u_e^{108/35}}\left[\int_0^x u_e^{27/7}\left(\frac{T_0}{T_e}\right)^{10/7} \times \left(\frac{\rho_r \mu_r}{\rho_0 \mu_0}\right) dx\right]^{4/5}. \quad (12)$$

A heat balance relating m_{hg} and m_{fc} is now written in the form suggested by Librizzi and Cresci [14], i.e.

$$m_{hg} c_{p_e}(T_{aw} - T'_{aw}) = m_{fc} c_{p_c}(T'_{aw} - T_{ci}) \quad (13)$$

or

$$\frac{T'_{aw} - T_{ci}}{T_{aw} - T'_{aw}} = \left(\frac{m_{hg}}{m_{fc}}\right)\left(\frac{c_{p_g}}{c_{p_c}}\right) \tag{14}$$

where $m_{fc} = u_c \rho_c L s$.

The left-hand side of equation (14) can be reorganized as $(1 - \eta)/\eta$ where η is the conventional film cooling effectiveness defined as $(T_{aw} - T'_{aw})/(T_{aw} - T_{ci})$. The term $(1 - \eta)/\eta$ is thus the ineffectiveness-to-effectiveness ratio.

Substitution of equation (12) in equation (14) with a slight manipulation yields

$$\frac{1-\eta}{\eta} = 0{\cdot}329a\left[\frac{Re_{g,x}^{0{\cdot}8}}{Re_{c,s}}\left(\frac{\mu_e}{\mu_c}\right)\left(\frac{c_{pe}}{c_{p_c}}\right)\right]\left(\frac{\rho_e}{\rho_0}\right)^{1/5} \times \left(\frac{\mu_0}{\mu_e}\right)^{1/5}\left(\frac{T_e}{T_0}\right)^{8/7}\frac{1}{x^{4/5}u_e^{108/35}} \times \left[\int_0^x u_e^{27/7}\left(\frac{T_0}{T_e}\right)^{10/7}\left(\frac{\rho_r \mu_r}{\rho_0 \mu_0}\right)\mathrm{d}x\right]^{4/5} \tag{15}$$

The first group of terms in the square brackets on the right side of equation (15) can be recognized as the parameter X, frequently used to correlate film cooling effectiveness data for incompressible, nonaccelerating flows, see equations (2, 4, 5). The other terms on the right side of equation (15) seem to correct X for the effects of compressibility and hot-gas acceleration.

Simplifying the integrand by taking $\rho_r \mu_r \sim \rho_0 \mu_0$ and expressing local velocities in terms of local Mach numbers and local density and viscosity ratios in terms of local pressure ratios, we obtain the final form

$$Y_1 = 0{\cdot}329aX_1 \tag{16}$$

where

$$Y_1 = \frac{1-\eta}{\eta}$$

$$X_1 = X\left[\left(\frac{p_e}{p_0}\right)^{\frac{1}{4}-\left(\frac{1+m}{4}\right)\left(\frac{\gamma-1}{\gamma}\right)}\frac{\sqrt{\left(1+\frac{\gamma-1}{2}M_a^2\right)}}{xMa^{27/7}} \times \int_0^x \frac{Ma^{27/7}}{\sqrt{\left(1+\frac{\gamma-1}{2}Ma^2\right)}}\mathrm{d}x\right]^{4/5}$$

and

$$X = \frac{Re_{g,x}^{0{\cdot}8}}{Re_{c,s}}\left(\frac{\mu_e}{\mu_c}\right)\left(\frac{c_{p_e}}{c_{p_c}}\right) = \frac{Re_{g,x}^{0{\cdot}8}}{Re_{c,s}}\left(\frac{Pr_g}{Pr_c}\right)\left(\frac{k_g}{k_c}\right).$$

It is evident that for the case of no hot-gas acceleration (Ma = constant) and low velocities ($p_e \sim p_0$), the parameter X_1 is identical to X. In essence, the correction due to acceleration amounts to replacing x in $Re_{g,x}$ by:

$$\left(\frac{p_e}{p_0}\right)^{\frac{1}{4}-\left(\frac{1+m}{4}\right)\left(\frac{\gamma-1}{\gamma}\right)}\frac{\sqrt{\left(1+\frac{\gamma-1}{2}Ma^2\right)}}{Ma^{27/7}} \times \int_0^x \frac{Ma^{27/7}\,\mathrm{d}x}{\sqrt{\left(1+\frac{\gamma-1}{2}Ma^2\right)}}$$

in conjunction with local values of $u_e \rho_e$. Stollery and El-Ehwany [3] propose the substitution of

$$\left(\frac{1+\frac{\gamma-1}{2}Ma^2}{Ma}\right)^4 \int_0^x \left(\frac{Ma}{1+\frac{\gamma-1}{2}Ma^2}\right)^4 \mathrm{d}x$$

for x in the parameter

$$\bar{x} = (Re_{g,x}/Re_{c,s}^{5/4})(\mu_g/\mu_c)^{5/4} = X^{5/4}(c_{p_c}/c_{p_g})^{5/4}.$$

However, no experimental data were provided to support this type of correction.

Equation (16) suggests the correlation of film cooling effectiveness data in the form of Y_1 vs. X_1. Accordingly, for a constant mixing coefficient, Y_1 is directly proportional to X_1. However, the experimental results presented herein show the mixing coefficient to vary with X_1, the free-stream turbulence intensity and the degree of hot-gas acceleration (convergence angle). Yet, the form of equation (16) correlates

the data markedly well and provides a valuable reference for understanding the effects of hot-gas acceleration and free-stream turbulence on film cooling effectiveness. This is discussed in detail in another section of this paper.

APPARATUS AND PROCEDURES

Test sections

Two types of test sections were utilized: a cylindrical constant-Mach-number test section and a series of rectangular converging test sections having convergence angles of 30, 45 and 60°. Both types of test sections are schematically illustrated in Fig. 1.

The cylindrical test section consisted of an electroformed nickel tube, 1·50-in I.D. with a 0·030-in wall thickness, approximately 8 in long Provision was made for either 360° film cooling or film cooling over a 90° sector. Two rows of wall thermocouples were installed with each row positioned in line with a gas inlet temperature probe. One row of thermocouples was centered at the mid-plane of the 90° sector, 0·0625-in wide film coolant slot, and the other row was diametrically opposite. Each row had thirteen thermocouples forming pairs with identical axial spacing. The spacing was 0·25 in near the film coolant slot, 0·5 in. in the center region and 1 in

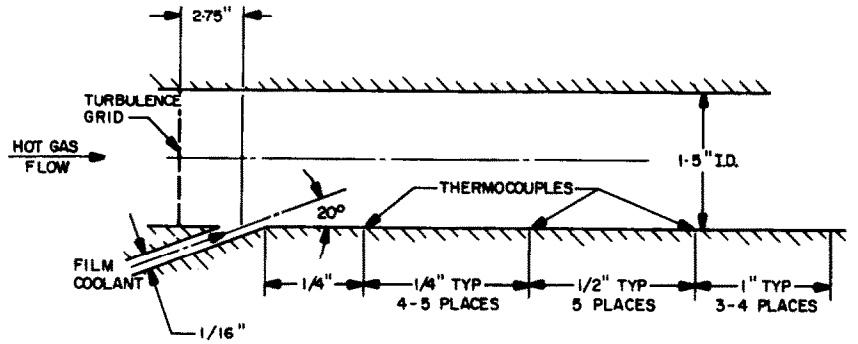

(a) CYLINDRICAL STRAIGHT

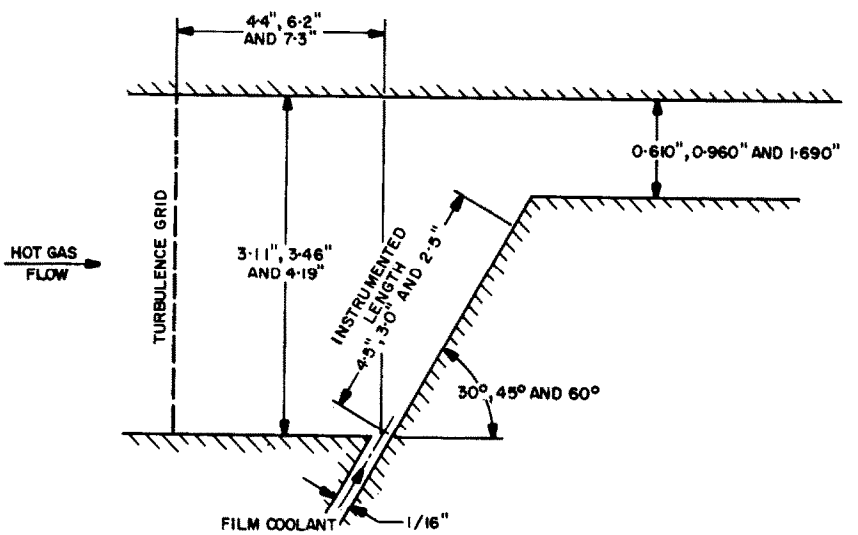

(b) TWO-DIMENSIONAL, CONVERGING; CHANNEL WIDTH = 1/2 IN

FIG. 1. Test section schematic.

near the test section outlet. Rounded exit nozzles were used to establish the test section Mach number.

The two-dimensional, accelerating flow test sections were formed from a set of common parts bolted to a circular adapter flange having a rectangular flow passage that matched the test section flow channel shape and housed turbulence-inducing grids. A flow transition section changed the flow cross section from a circular 2 in pipe to the required rectangular cross section upstream of the test section flange. Each test section consisted of two flow channels 0·5-in wide separated by a thin stainless steel plate. A 0·0625 × 0·5 in constant area slot provided a spanwise-uniform film coolant flow to one of the channels parallel to the ramp surface (Fig. 1b). The calculated thickness of the side-wall boundary layer at the film coolant slot was negligible relative to the slot width.

Calorimeters were made of 0·0104-in thick copper sheet bent around the corners of grooved aluminium ramp pieces. The 0·0625-in deep by 0·375-in wide grooves in the ramp pieces provided space for the thermocouples, which were fastened to the back side of the calorimeter. These grooves also insulated the back face of the calorimeter from heat conduction. Thermocouple spacing was 0·5 in for the 30° ramps, 0·375 in for the 45° ramps, and 0·25 in for the 60° ramp, starting in each case one space downstream of the exit of the slot. Ten, nine, and ten thermocouples were used in each calorimeter for the 30, 45 and 60° ramps, respectively. Each of the two-dimensional test-section flow channels consisted of a constant area entrance section following the turbulence grid, a convergent section, and a constant-area sonic throat (Fig. 1b).

Instrumentation

Premium grade, Chromel–Alumel thermocouple wire was used to measure gas and wall surface temperatures. Transient gas temperatures were measured using 0·005-in dia. exposed wire thermocouples supported ten wire diameters from the junction by a metallic sheath and magnesia insulation (Thermoelectric Company-"Ceramo" type wire). These gas measuring thermocouples were placed upstream of the film coolant slot but downstream of the turbulence grid and extended into the gas stream 0·25 in (mid channel for the two dimensional test sections). The minimum transient response of these thermocouples to the gas temperature transient was calculated to be 5 ms.

The cylindrical test section thermocouples were fabricated using 0·005-in dia. wire with double junctions fusion welded in close proximity (<0·03125 in) on the outer surface of the electro-formed nickel test section. The wires were led laterally around the test section for some distance in contact with the equal-temperature surface to minimize heat conduction error.

The calorimeter surfaces of the accelerating flow test sections were equipped with 0·003-in dia. thermocouple wire. A scratch and peen operation was used to secure the wires to the thin (0·010-in thick) copper calorimeter pieces. With this technique the wires were laid in close parallel grooves scratched in the surface and the edges of the copper groove were pressed back over the wire, mechanically locking it in place. Because the effective junction was formed at some distance under the groove, heat conduction from the junction along the wire was minimized.

The thermocouples from the various test sections were connected to the recording system using insulated gold-plated pin connectors. Male and female pin connectors on the thermocouple harness of Chromel–Alumel wire terminated in an ice-bath. Double cold junction terminations were used in the ice bath so that copper–copper lead wire from the ice bath could be used. The copper wires were connected to shielded copper conductors at a junction board a few feet from the ice bath. The shielded conductors carried the thermocouple signals directly to a digitizer approximately 1000 ft away.

The time transient outputs from inlet gas

and wall temperature measuring thermocouples were gathered by a Beckman 210 digital data acquisition system in conjunction with a magnetic tape recording facility. The temperature data from each of fifty channels could be sampled every 0·0117 s and recorded in digital form with an accuracy of approximately one part in 4000.

Wiancko pressure transducers, calibrated using Heise gauges, were used to monitor and record test section and flow facility pressures both before and during the tests. The pressures were recorded on continuous strip charts using Honeywell–Brown recorders operating at 0·25-in/s chart speed and having 0·5 per cent full-scale calibration accuracy.

Hot-gas facility

A hot-gas facility supplied 1000°F nitrogen at flowrates and pressures up to 3·5 lb/s and 1000 lb/in^2, respectively. The facility consisted of a pressure-regulated, ambient temperature nitrogen supply and an electrically heated, "pebble-bed-type" regenerative heat exchanger. A 2-in dia., double burst diaphragm acted as a hot-gas valve at the outlet of the heat exchanger. This valve had an effective opening time of 1 ms. A 1-ft long, 2-in pipe spool, at the outlet of the hot-gas valved housed a fast-response Photocon pressure transducer and fast-response gas temperature probes. The spool also adapted the facility to the various test sections employed.

The mass flowrate of the gas was controlled by the main pressure regulator. Flowrates were calculated from measured gas pressures and temperatures and known exit throat areas. Ambient-temperature (70°F) gaseous film coolant was supplied by an auxiliary pressure regulating system. Film coolant flowrates were controlled by set supply pressures and calibrated sonic orifices.

Turbulence grids

Turbulence grids were designed on the basis of available criteria and correlations [23–27] which cover the geometrical conditions of this study. The grids consisted of crossed rows of tubing or wire screen arranged to induce turbulence intensities of 3·2, 12 and 22 per cent at the film coolant slot of the cylindrical test section.

While the turbulence intensities were not experimentally checked, the values mentioned are average of at least two methods of calculation. With the difference between methods being no more than 1 per cent intensity, the indicated intensity levels are good estimates for comparative purposes particularly at the higher levels relative to the case of low or negligible free-stream turbulence.

For the accelerated-flow test sections, the 12- and 22-per cent grids were used. The grids were at a fixed position, and as the convergence angle of the test section was increased, the distance between the grid and the start of convergence (where the film coolant was injected) also increased. This resulted in a decay of the estimated free-stream turbulence intensity at the film coolant slot as the convergence angle was increased. For example, the generated 12-per cent turbulence level decayed to 8·8, 7·0 and 6·4 per cent at convergence angles of 30, 45 and 60°, respectively.

Data reduction

As previously described, the gas and wall transient temperature data were recorded on a Beckman 210 digital system. These data were reduced, using two separate computer programs, to obtain two basically different types of information: steady-state wall temperatures and heat-transfer coefficients. The steady-state wall temperatures were reduced further into film cooling effectiveness values.

The digitized temperature data, which were available in analog form on Brush recording charts, were examined to determine a time interval for each run which represented the steady-state temperature conditions. The digitized data during this time interval were processed for each run using an unpacking and temperature scaling program to obtain the

temperature values. These temperatures were listed by the computer both as an individual time-value series and as average values for the chosen time series. Temperatures were always constant enough during a time interval so that the average value could be used for any given run. These steady-state wall temperatures (T'_{aw}) were used to determine the film cooling effectiveness defined by equation (2).

The calculation of film cooling effectiveness required the adiabatic wall temperatures with and without film cooling at otherwise identical mainstream flow conditions. Hence the simultaneous reference measurements made with the film-cooled and nonfilm-cooled channels in the test sections yielded the required information automatically. The adiabatic wall temperature data in the form of η were correlated vs. the flow parameter X_1 (or X) defined in conjunction with equation (16).

The gas transport properties in X were evaluated at the mainstream gas temperature, while those for the film coolant were evaluated at its injection temperature. The mainstream gas Reynolds number was evaluated at the local position as denoted by the subscript x taken parallel to the flow along the wall.

For the accelerating flow case, the hot-gas Reynolds numbers were based on the local superficial mass velocity as determined by a one-dimensional flow model. Such model is valid along a converging wall for the early part of convergence (Mach numbers up to 0·5) where the wall-temperature measurements were taken.

The constant-Mach-number film cooling data were correlated vs. X in the forms suggested by equations (2) and (4) with the free-stream turbulence intensity as a parameter. The film cooling effectiveness data for the accelerating-flow test sections were similarly correlated vs. X_1, i.e. the form of equation (16). The results are presented and discussed in a subsequent section of this paper.

The Brush recordings were also used to choose a time interval of the transient temperature response for calculation of heat-transfer coefficients without film cooling. The model used for this purpose stipulated a thin-plate calorimeter of high thermal conductivity, so that the heat-transfer coefficients could be calculated from the relation:

$$h(T_{aw} - T_w) = \rho_w c_{p_w} \xi (\mathrm{d}T_w/\mathrm{d}t). \qquad (17)$$

The heat-transfer coefficients thus obtained were used to correct η for lateral conduction in the accelerated-flow test sections. The lateral conduction in the cylindrical test section was negligible. Axial conduction was negligible in all cases.

The lateral-conduction error analysis assumed a constant heat-transfer coefficient at a given location and a constant-temperature heat sink. This allowed the solution of the fin-conduction equation for the correct adiabatic wall temperature.

RESULTS AND DISCUSSION

Eighty-two runs were conducted with gaseous nitrogen as the hot gas and film coolant. Twenty-eight runs were with the straight cylindrical test section and fifty-four runs were with the accelerated-flow, two-dimensional test sections.

For most of the constant-Mach-number runs, a 90° sector film coolant slot was used. One run was conducted with a 360° slot resulting in excellent agreement with 90° slot cooling at a comparable coolant-to-gas flowrate ratio. Film cooling effectiveness data were obtained at free-stream turbulence intensities of 3·2, 12 and 22 per cent, nominal film coolant flowrates of 2, 4 and 8 per cent of the hot-gas flowrate, and nominal hot-gas Mach numbers of 0·1, 0·3 and 0·5. The injection-to-free-stream velocity ratio thus varied from 0·17 to 0·67.

Similar data at various degrees of hot-gas acceleration (convergence angles of 30, 45 and 60°) were obtained at free-stream turbulence intensities between 7·0 and 14 per cent, inlet hot-gas Mach numbers of 0·115, 0·163 and 0·242, and nominal film coolant flowrates of 1, 2 and 4

per cent of the hot-gas flowrate per channel. The corresponding injection-to-free-stream velocity ratios at the film coolant slot were in the range of 0·19 to 0·90.

Effect of free-stream turbulence intensity

Correlated data for the cylindrical test section (constant-Mach-number data) are given in Fig. 2 in the form of η vs. X_1 for turbulence intensities of 3, 12 and 22 per cent. For a given turbulence level, the effects of variable film-coolant flowrate and hot-gas Mach number seem to be adequately correlated by the parameters shown. Comparison of data at various turbulence levels indicates that the effect of turbulence on film cooling effectiveness is considerable (Fig. 2); the higher the turbulence intensity at the point of film-coolant injection, the lower is the film cooling effectiveness in the entire range of X_1 investigated.

Inspection of Fig. 2 reveals that for a given turbulence level, at least three constants are required to express the results in the form of equation (2) for the entire range of X_1 investigated. Alternative plots of the data in the form suggested by equation (16) are given in Fig. 3. Plotted here is Y_1, or the film cooling ineffectiveness-to-effectiveness ratio vs. X_1, with the dotted lines representing the predictions of equation (16) for various mixing coefficients.

According to equation (16), once a constant mixing coefficient is established, a logarithmic plot of Y_1 vs. X_1 (Fig. 3) should yield a straight line with a slope of one. This seems to be the case at large values of X_1 (away from the film coolant injection point) with the data approaching this condition at slopes higher than one. However, only two constants are required to express the results in the form of equation (16) for the entire range of X_1 investigated.

An insight into the effect of turbulence intensity on film cooling effectiveness is provided when the mixing coefficients approached by the data at various turbulence levels are compared. For example, at an estimated free-

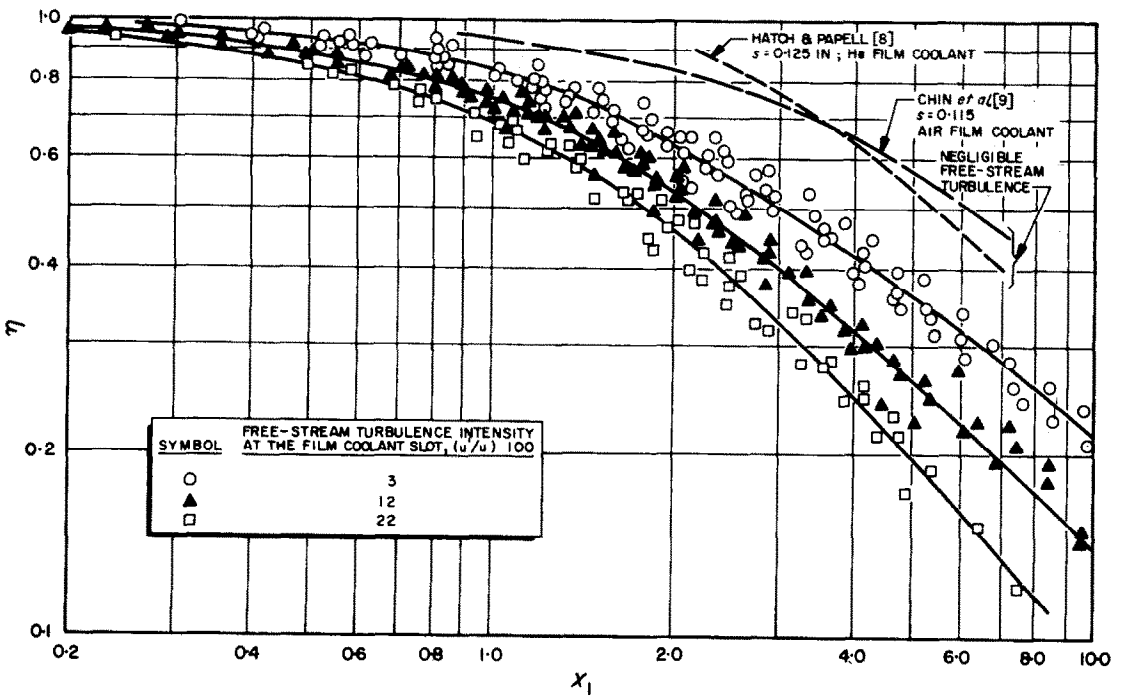

FIG. 2. Effect of free-stream turbulence intensity on film cooling effectiveness in nonaccelerating flow: $0{\cdot}17 < u_c/u_g < 0{\cdot}67$.

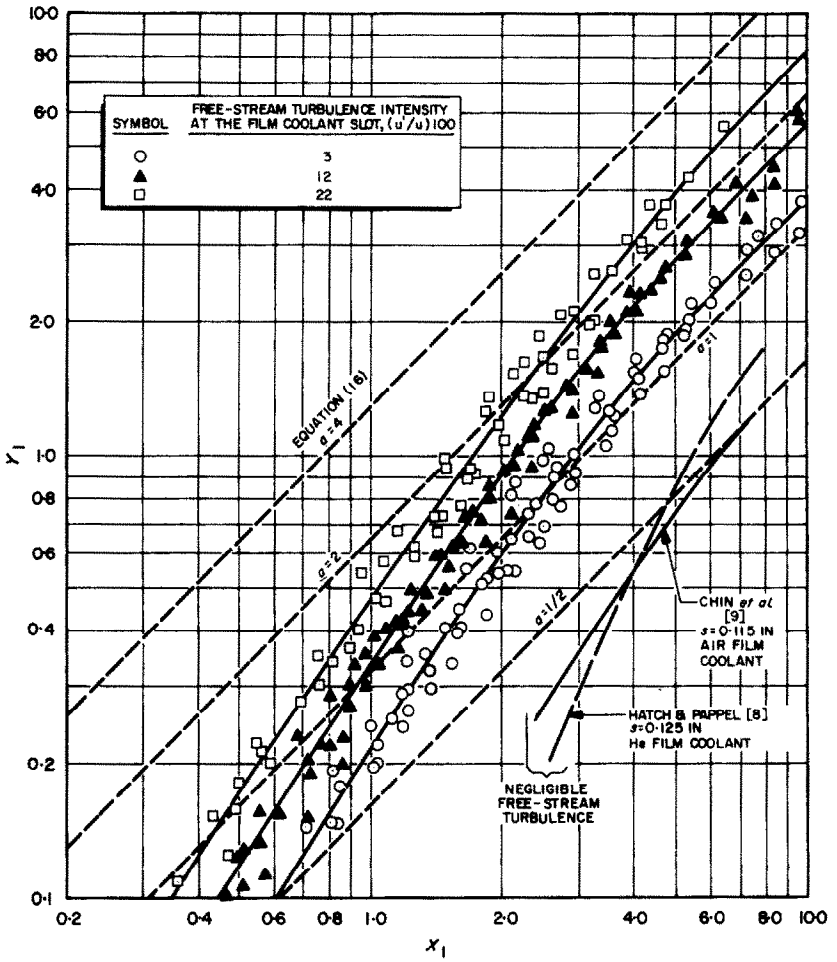

FIG. 3. Nonaccelerated flow results in the form suggested by equation (16).

stream turbulence intensity of 3 per cent (Fig. 3), a constant mixing coefficient slightly over one is established for $X > 4$ and the slope of the data is one in that range [as predicted by equation (16)]. Similarly, mixing coefficients of approximately 2 and 3 are established at turbulence intensities of 12 and 22 per cent, respectively. The higher the turbulence intensity, the higher is the mixing coefficient, i.e. the larger the effective quantity of hot gas mixed with the film coolant. Thus, the effect of increased turbulence is to extend the mixing zone into the bulk of the hot-gas stream.

The application of the results given in Fig. 2 or 3 to the combustion zones of high-temperature combustors requires knowledge of the combustion-induced turbulence intensity involved. Such information is currently available for only a few propellant combinations.

For example, with the propellant combination of liquid oxygen–gaseous hydrogen, turbulence intensities in the range of 10–5 per cent are reported for distances of 2–8 in from the injector face. These results are based on optical tracer measurements [28]. With the propellant combination of N_2O_4/50 per cent N_2H_4–50 per cent unsymmetrical dimethyl hydrazine, turbulence intensities in the range of 20–15 per cent

were deduced [13] from the related measurements of heat transfer to immersed throat-tubes placed 6 and 23 in from the injector face, respectively. No similar information is available with other propellant combinations.

Effect of hot-gas acceleration rate

Correlated data for the two-dimensional test sections (accelerated flow data) are given in Figs. 4 and 5 for turbulence intensities of 6·4–8·8 and 10–14 per cent, respectively. In each case, the film-cooling effectiveness is plotted vs. X_1 on log–log coordinates, with the convergence angle as a parameter. A corresponding curve at a turbulence intensity of 12 per cent with no hot-gas acceleration (Fig. 2) is superimposed on the data of Fig. 5 for comparison.

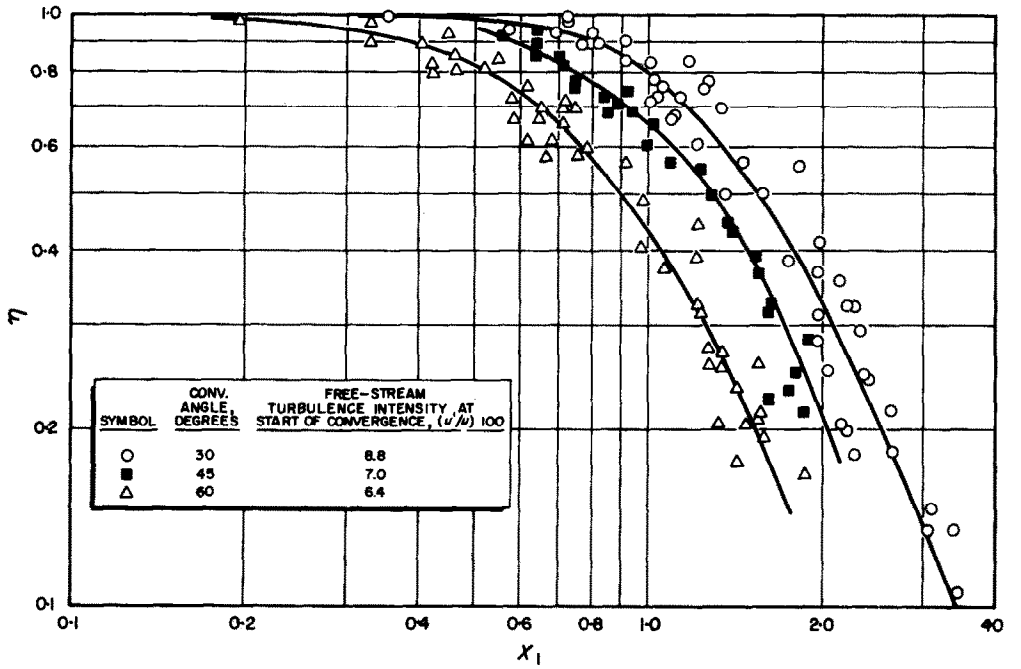

FIG. 4. Effect of hot-gas acceleration rate on film cooling effectiveness at estimated free-stream turbulence intensities of 6·4–8·8 per cent; $0{\cdot}19 < u_c/u_{g,s} < 0{\cdot}90$.

For a given turbulence level, comparison of the results at convergence angles of 30, 45 and 60° indicates that the higher the rate of acceleration (convergence angle) the lower is the film cooling effectiveness in the entire range of X_1 investigated. In this respect the effect of acceleration rate is equivalent to that of the free-stream turbulence intensity (Fig. 2). However, comparison to the case of no acceleration (Fig. 5) indicates that a mild rate of hot-gas acceleration, e.g. convergence angle of 30° improves the film cooling effectiveness at $X_1 < 0{\cdot}9$ (close to the film coolant injection point). This is apparently due to a favorable hydrodynamic force provided by the accelerating gas adhering the film coolant to the wall upon injection. However, the limited beneficial effect of hot-gas acceleration (at $X_1 < 0{\cdot}9$) tends to disappear at higher rates of hot-gas acceleration, e.g. at a convergence angle of 60°.

In a subsequent step to this observation, the effect of hot-gas acceleration rate on dry-wall heat-transfer coefficients (without film cooling) was also examined. For each convergence angle, dry-wall heat-transfer coefficients were determined from related slopes of temperature histories taken at the beginning of each run so as

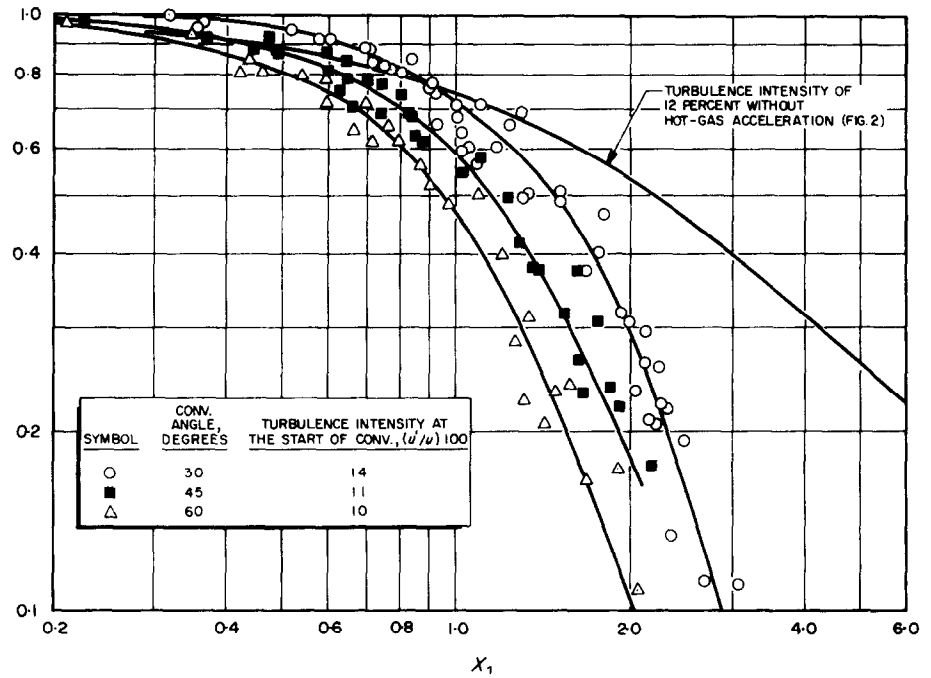

FIG. 5. Effect of hot-gas acceleration rate on film cooling effectiveness at estimated free-stream turbulence intensities of 10–14 per cent; $0{\cdot}19 < u_c/u_{g,s} < 0{\cdot}90$.

to minimize the lateral conduction error. In this manner all heat-transfer coefficients were based on essentially-ambient wall temperatures (and an essentially-constant gas temperature) allowing direct comparison for ascertaining the effect of hot-gas acceleration rate.

Pertinent results in the form of Nu_x vs. $Re_{g,x}$ are given in Fig. 6 for convergence angles of 30, 45 and 60°. For clarity, the combined log–log plot presents best-straight-line fits only. As shown (Fig. 6), the slopes of the heat-transfer lines seem to increase with convergence angle, revealing the type of cross-over phenomenon observed at the sonic-point of high-temperature combustors [29]. Furthermore, within the range of $Re_{g,x}$ investigated, the dry-wall heat-transfer rates at a convergence angle of 60° are lower than at a convergence angle of 30° (Fig. 6), so that the observed degradation in film cooling effectiveness at the higher convergence angles could not have resulted from the related effect on dry-wall heat-transfer coefficients. Apparently, enhanced mixing of film coolant and hot gas is the controlling mechanism.

The observed detrimental effect of high acceleration rates on film cooling effectiveness seems to be in line with results previously obtained with external-flow configurations. For example [30], improved film cooling effectiveness was encountered with noncircular, immersed throat-bodies in comparison to circular throat tubes [11] having the same cross-flow dimension. Changing the throat-body shape in external-flow configurations is analogous to varying the convergence angle in internal-flow situations [31].

For a given convergence angle, cross-comparison of the results given in Fig. 4 and 5 shows that at the higher rates of hot-gas acceleration the effect of free-stream turbulence at the point of film-coolant injection (start of convergence) is insignificant. In fact, at a convergence angle of 60°, the data obtained at turbulence intensities of 6·4 and 10 per cent could be combined and

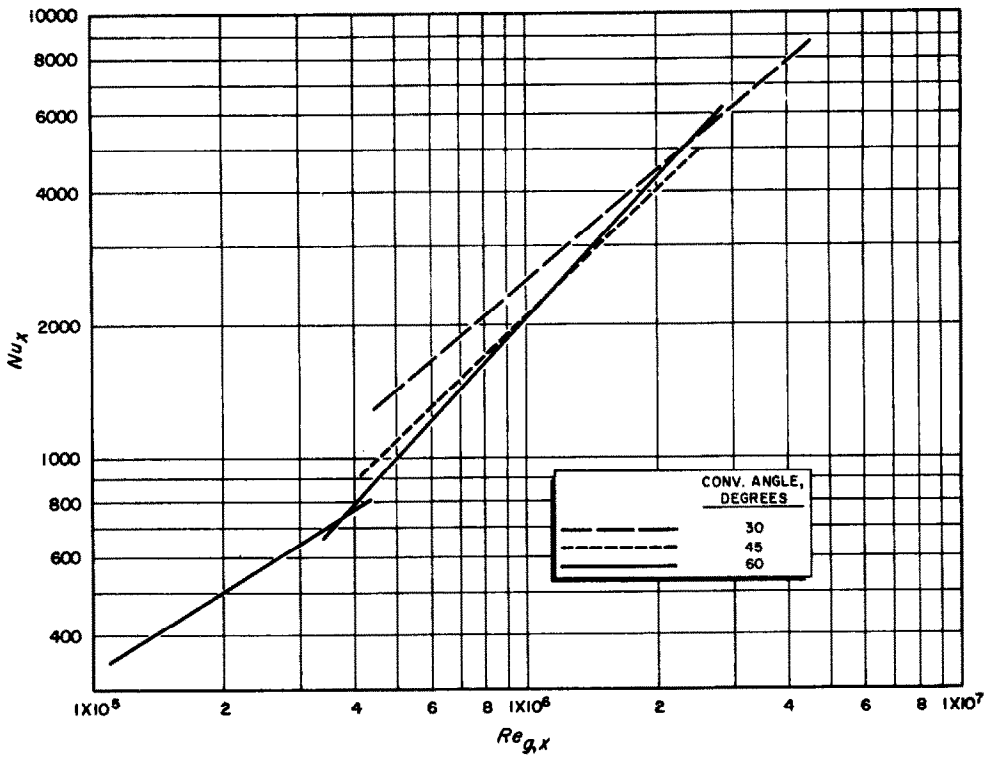

FIG. 6. Effect of convergence-angle on dry-wall Nusselt numbers.

represented by a single curve. Three explanations can be offered for this observation: an adverse effect of gas acceleration on free-stream turbulence, an acceleration-induced turbulence which overrides the initial turbulence intensity (at the start of acceleration) or hot-gas separation at the film coolant slot due to sharp turning of the flow [32]. Unfortunately, local measurements of free-stream turbulence were not available to support any of the explanations offered.

Alternative plots of the accelerated-flow data in the form suggested by equation (16) are given in Figs. 7 and 8 for turbulence intensities of 6·4–8·8 and 10–14 per cent, respectively. The dotted lines represent the predictions of equation (16) for various mixing coefficients.

As shown (Figs. 7 and 8), a constant mixing coefficient is not established in the range of X_1 investigated, i.e. the mixing zone in the accelerated-flow case propagates continuously toward the centerline of the hot-gas stream. Furthermore, the ineffectiveness-to-effectiveness ratio is linear with X_1 on log–log coordinates with slopes of linearity larger than one, i.e. for a given turbulence intensity and hot-gas acceleration rate, one constant is sufficient to express the results in the form of equation (16) provided that X_1 is taken to a power between 2·5 and 3·0. Thus, the form of equation (16), or Figs. 7 and 8, is preferable to that depicted by Figs. 4 and 5.

CONCLUSIONS AND RECOMMENDATIONS

The free-stream turbulence and the rate of hot-gas acceleration have considerable effects on film cooling effectiveness. Both have to be considered when applying film cooling to high-temperature combustors.

Without hot-gas acceleration, the higher the free-stream turbulence intensity (at the injection

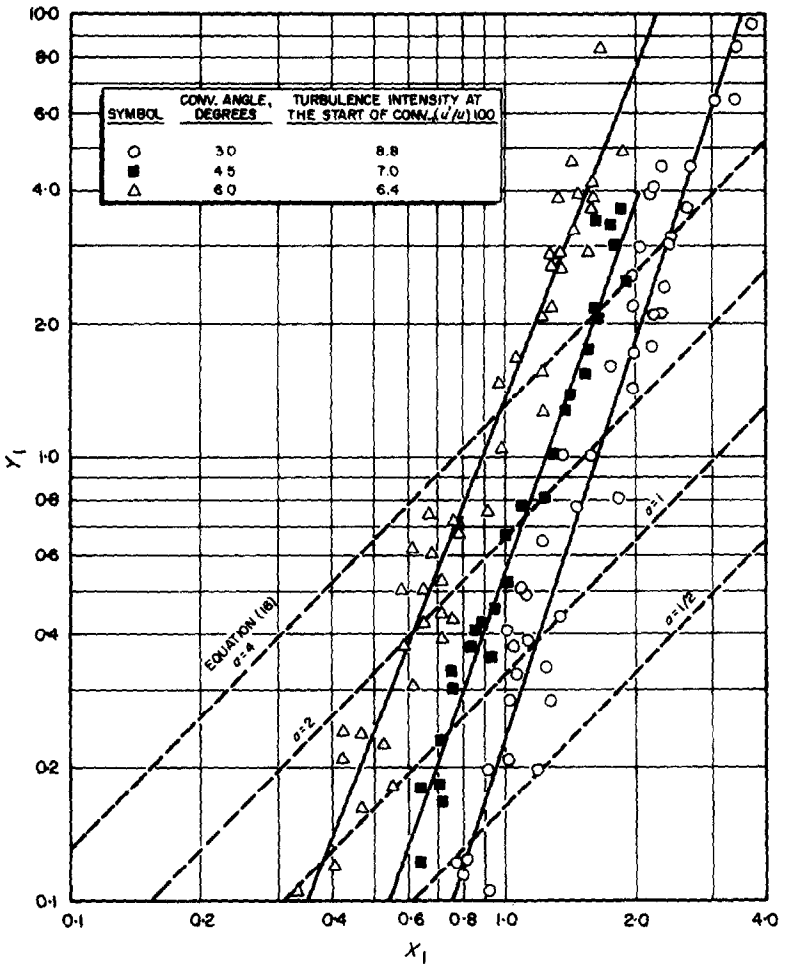

FIG. 7. Straight line fits of the data of Fig. 4 in accordance with equation (16).

point of the film coolant), the higher is the effective quantity of hot-gas mixed with the film coolant. This is reflected by the successful correlation of experimental data with a model which does not restrict the amount of hot gas mixed with the film coolant. While the degree of mixing (mixing coefficient) is increasing with distance from the film-coolant injection point, it does reach a constant value beyond a certain distance. The value reached depends upon the free-stream turbulence intensity, e.g. mixing coefficients between one and three for estimated turbulence intensities between 3·2 and 22 per cent (Fig. 3).

With increasing rates of hot-gas acceleration, the effect of free-stream turbulence at the start of convergence (injection point of the film coolant) is not as significant. However, the increase in the acceleration rate itself has a detrimental effect on film cooling effectiveness along converging walls, particularly at larger distances from the film coolant slot (or lower film coolant flowrates).

Close to the film coolant slot ($X_1 < 0{\cdot}9$), a mild rate of hot-gas acceleration, e.g. convergence angle of 30°, improves the film cooling effectiveness. However, at $X_1 > 0{\cdot}9$, the effect of hot-gas acceleration rate is equivalent to that of the free-stream turbulence in nonaccelerating

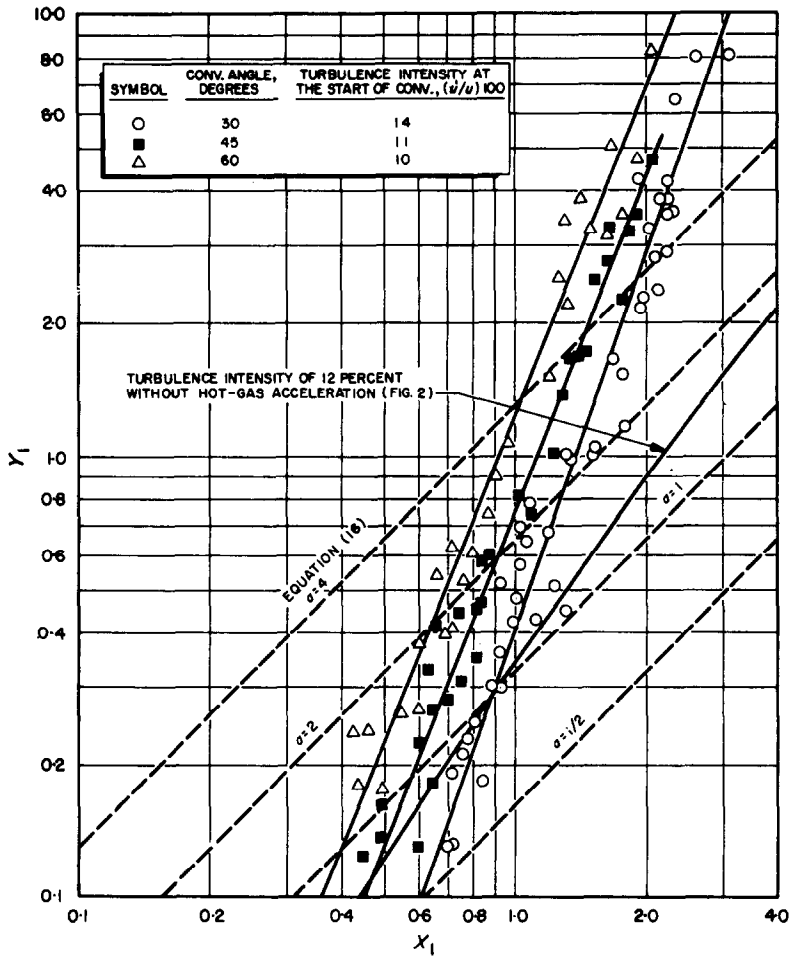

FIG. 8. Straight line fits of the data of Fig. 5 in accordance with equation (16).

flow, and at the higher rates of hot-gas acceleration, e.g. convergence angle of 60°, the limited beneficial effect of hot-gas acceleration (at $X_1 < 0{\cdot}9$) disappears.

The degree of mixing (mixing coefficient) in all cases of hot-gas acceleration increases with distance from the film-coolant slot without reaching a constant value, i.e. the effective mixing zone in the accelerated flow case propagates continuously toward the centerline of the hot-gas stream, and in this respect, the effect of increased rates of hot-gas acceleration is more severe than that of the free-stream turbulence.

Regardless of whether or not a constant mixing coefficient was reached, all data correlate markedly well in a form suggested by a newly derived mixing model which considers compressibility and allows for a variable degree of mixing. The advantages of correlating the data in the form of Y_1 vs. X_1 (on log–log coordinates) are particularly obvious for the case of hot-gas acceleration (Figs. 7 and 8).

Inspection of the variation of the dry-wall heat-transfer coefficients with the rate of hot gas acceleration indicates that the detrimental effect of the latter on film cooling effectiveness is not due to increased dry-wall heat-transfer

coefficients. In fact, the dry-wall Nusselt numbers (based on x) generally decreased with increasing convergence angle within the range of $Re_{g,x}$ investigated. Enhanced mixing is apparently the mechanism by which the increase in convergence angle decreases the film cooling effectiveness, particularly toward the larger values of X_1.

Local measurements of free-stream turbulence intensity are badly needed to determine a possible interaction between the hot-gas acceleration rate and the free-stream turbulence intensity. Such measurements are also required to determine the extent of turbulence induced by the injection of the film coolant (with and without hot-gas acceleration).

Another effect yet to be determined is that of dissimilar gases, i.e. film coolants having molecular weights greater and smaller than that of the hot-gas at various degrees of hot-gas acceleration and free-stream turbulence levels. This is currently being investigated as a follow-on to the research program reported herein.

ACKNOWLEDGEMENTS

The authors wish to acknowledge Mr. W. Bose for fine experimental support and Mr. J. Sabol for his excellent help in reducing the large amount of data acquired.

REFERENCES

1. J. P. HARTNETT, R. C. BIRKEBAK and E. R. G. ECKERT, Velocity distribution, temperature distributions, effectiveness and heat transfer in cooling of a surface with a pressure gradient, *International Developments in Heat Transfer*, Vol. IV, pp. 682–689. Am. Soc. Mech. Engrs, New York (1961).
2. R. A. SEBAN and L. H. BACK, Effectiveness and heat transfer for a turbulent boundary layer with tangential injection and variable free-stream velocity, *J. Heat Transfer* **84**, 235–244 (1962).
3. J. L. STOLLERY and A. A. M. EL-EHWANY, A note on the use of boundary-layer model for correlating film-cooling data, *Int. J. Heat Mass Transfer* **8**, 55–85 (1965).
4. D. B. SPALDING, Prediction of adiabatic wall temperatures in film-cooling systems, *AIAA Jl* **3**, 965–967 (1965).
5. A. E. SAMUEL and P. N. JOUBERT, Film cooling of an adiabatic flat plate in zero pressure gradient in the presence of a hot mainstream and cold tangential secondary injection, *J. Heat Transfer* **87**, 409–418 (1965).
6. M. TRIBUS and J. KLEIN, Forced convection from nonisothermal surfaces, in *Heat Transfer Symposium*, pp. 211–235, Engineering Research Institute, University of Michigan, Ann Arbor, Michigan (1953).
7. J. P. HARTNETT, R. C. BIRKEBAK and E. R. G. ECKERT, Velocity distributions, temperature distributions, effectiveness and heat transfer for air injected through a tangential slot into a turbulent boundary-layer, *J. Heat Transfer* **83**, 293–306 (1961).
8. R. A. SEBAN and L. H. BACK, Velocity and temperature profiles in turbulent boundary layers with tangential injection, *J. Heat Transfer* **84**, 45–54 (1962).
9. J. E. HATCH and S. S. PAPELL, Use of a theoretical flow model to correlate data for film cooling or heating an adiabatic wall by tangential injection of gases of different fluid properties, NASA TN D-130 (1959).
10. J. H. CHIN, S. C. SKIRVIN, L. E. HAYES and F. BURGGRAF, Film cooling with multiple slots and louvers, *J. Heat Transfer* **83**, 281–292 (1961).
11. E. TALMOR, Film cooling of small diameter throat tubes, *Chem. Engng Prog. Symp. Ser.* **62**(64), 216–224 (1966).
12. C. E. WOOLDRIDGE and R. J. MUZZY, Boundary layer turbulence measurements with mass addition and combustion, *AIAA JI* **4**, 2009–2016 (1966).
13. E. TALMOR, Turbulence determination and blockage correction for immersed cylinder heat transfer at high Reynolds numbers, *A.I.Ch.E. Jl* **12**, 1092–1097 (1966).
14. J. LIBRIZZI and R. J. CRESCI, Transpiration cooling of a turbulent boundary layer in an axisymmetric nozzle, *AIAA Jl* **2**, 617–624 (1964).
15. N. NISHIWAKI, M. HIRATA and A. TSUCHIDA, Heat transfer on a surface covered by cold air film, *International Developments in Heat Transfer*, Vol. IV, pp. 675–681. Am. Soc. Mech. Engrs, New York (1961).
16. G. T. CHAPMAN, Total boundary-layer mass flow with mass transfer at the wall, *AIAA Jl* **4**, 1688–1689 (1966).
17. S. S. KUTATELADZE and A. I. LEONTEV, The heat curtain in the turbulent boundary layer of a gas, *High Temperature* **1**, 250–258 (1963).
18. R. J. GOLDSTEIN, G. SHAVIT and T. S. CHEN, Film-cooling effectiveness with injection through a porous section, *J. Heat Transfer* **87**, 353–361 (1965).
19. R. J. GOLDSTEIN, R. B. RASK and E. R. G. ECKERT, Film cooling with helium injection into an incompressible air flow, *Int. J. Heat Mass Transfer* **9**, 1341–1350 (1966).
20. S. S. KUTATELADZE and A. I. LEONTEV, *Turbulent Boundary Layers in Compressible Gases*, pp. 67–71. Academic Press, New York (1964).
21. A. I. LEONTEV, Heat and mass transfer in turbulent boundary layers, *Adv. Heat Transf.* **3**, 62–80 (1966).
22. I. E. BECKWITH and J. J. GALLAGHER, Local heat transfer and recovery temperatures on a yawed cylinder at a Mach number of 4·15 and high Reynolds numbers, NASA TR R-104 (1961).
23. J. O. HINZE, *Turbulence*, pp. 142–245. McGraw-Hill, New York (1959).
24. S. J. KLINE, A. V. LISIN and B. A. WAITMAN, An experimental investigation of the effect of free-stream turbulence on the turbulent boundary layer growth, Report MD-2, Department of Mechanical Engineering, Stanford University (May 1958).
25. S. LOEZOS, Experimental study of the decay of turbulence, Report 2238, David Taylor Model Basin, Department of the Navy, Washington, D.C. (June 1966).

26. A. L. KISTLER and T. VREBALOVICH, Grid turbulence at large Reynolds numbers, *J. Fluid Mech.* **26**(1), 37–47 (1966).
27. G. COMTE-BELLOT and S. CORRSIN, The use of a contraction to improve the isotropy of grid-generated turbulence, *J. Fluid Mech.* **25**(4), 667–682 (1966).
28. M. HERSCH, Experimental method of measuring Intensity of turbulence in a rocket chamber, *ARS Jl* **31**, 39–45 (1961).
29. E. TALMOR, Sonic-point heat transfer at various degrees of upstream acceleration, *Chem. Engng. Prog. Symp. Ser.* **64**(82), 231–239 (1968).
30. E. TALMOR, Heat transfer to noncircular throat bodies, in *Proceedings of the Third International Heat Transfer Conference*, Vol. I, pp. 77–84. Am. Inst. Chem. Engrs, New York (1966).
31. E. TALMOR, Effect of pressure gradient on sonic-point heat transfer, *A.I.Ch.E.Jl* **1**, 127–134 (1968).
32. L. H. BACK, P. F. MASSIER and R. F. CUFFEL, Some observations on reductions of turbulent boundary layer heat transfer in nozzles, *AIAA Jl* **4**, 2226–2229 (1966).

Résumé—On présente une étude expérimentale et théorique du refroidissement par film gazeux pour différentes valeurs de l'accélération du gaz chaud et une intensité variable de la turbulence de l'écoulement amont. La valeur de l'accélération variait avec l'angle de convergence (0, 30, 45 et 60°) et l'intensité de la turbulence de l'écoulement libre (3,2 à 22 pour cent) était modifiée par des grilles placées perpendiculairement à l'écoulement et en amont de la fente pour le refroidissement par film. L'écoulement de gaz chaud consistait en azote à 540°C en employant pour le refroidissement par film de l'azote à température ambiante (21°C).

On donne des résultats quantitatifs pour la diminution de l'efficacité de refroidissement par film le long des parois convergentes par suite d'une augmentation de la turbulence de l'écoulement libre et de l'angle de convergence des parois. Les résultats sont corrélés sous une forme suggérée par un modèle de mélange obtenu récemment, qui tient compte de la compressibilité et permet un degré variable de mélange.

Zusammenfassung—Es wird von einer experimentellen und analytischen Untersuchung berichtet über Filmkühlung mit Gasen bei verschiedenen Heissgasbeschleunigungen und verschiedenen Freistromturbulenzintensitäten. Die Beschleunigung wurde durch den Konvergenzwinkel verändert (0, 30, 45 und 60 Grad), die Freistromintensität (3,2 bis 22 prozent) wurde durch quer angeströmte Gitter, die stromaufwärts vom Filmkühlschlitz angebracht waren, variiert. Der Heissgasstrom bestand aus Stickstoff von 538°C, das Kühlmittel war Stickstoff von Umgebungstemperatur (21°C).

Quantitative Ergebnisse über schädliche Einflüsse der erhöhten Freistromturbulenz und des Wandkonvergenzwinkels auf die Wirksamkeit der Filmkühlung an konvergierenden Wänden sind angegeben. Eine Korrelation liess sich in der Form erreichen, wie sie in einem neu abgeleiteten Mischmodell vorgeschlagen wird, das die Kompressibilität berücksichtigt und verschiedene Mischungsgrade zulässt.

Аннотация—Представлено экспериментальное и аналитическое исследование пленочного охлаждения при различных отрицательных градиентах давления горячего газа и различной степени турбулентности свободного потока. Ускоряющийся поток создавался с помощью суживающихся сопел (углы раствора 0, 30, 45 и 60°), а степень турбулентности свободного потока (3,2–22%) изменялась с помощью решеток, расположенных вверх по потоку от щели, через которую вводится охладитель. В качестве охладителя и теплоносителя использовался азот с температурой 70°F и 1000°F, соответственно.

Приводятся количественные результаты, свидетельствующие о снижении эффективности защиты стенок сопла с помощью пленочного охлаждения при возрастании степени турбулентности свободного потока и угла раствора. Данные скоррелированы с помощью недавно разработанной применимой к различным степеням перемешивания модели смешения, в которой учитывается сжимаемость.